



HHS Public Access

Author manuscript

Biol Psychiatry Cogn Neurosci Neuroimaging. Author manuscript; available in PMC 2023 June 01.

Published in final edited form as:

Biol Psychiatry Cogn Neurosci Neuroimaging. 2022 June ; 7(6): 588–597. doi:10.1016/j.bpsc.2020.08.014.

Differences in diffusion weighted imaging and resting-state functional connectivity between two culturally distinct populations of prairie vole

Richard Ortiz¹, Jason R. Yee², Praveen P. Kulkarni², Nancy G. Solomon³, Brain Keane⁴, Xuezu Cai², Craig F. Ferris^{2, #}, Bruce S. Cushing^{1, *, #}

¹Department of Biological Sciences, University of Texas at El Paso, El Paso, TX, 79968

²Department of Psychology, Center for Translational Neuroimaging, Northeastern University, Boston, MA, 02115

³Department of Biology, Miami University, Oxford, OH 45056, USA

⁴Department of Biological Sciences, Miami University, Hamilton, OH 45011, USA

Abstract

Background: We used the highly prosocial prairie vole to test the hypothesis that higher-order brain structure, microarchitecture and functional connectivity, would differ between males from populations with distinctly different levels of prosocial behavior. Specifically, Males from Illinois (IL), who display high levels of prosocial behavior and F1 males from Kansas dams and Illinois males (KI), which display the lowest level of prosocial behavior and higher aggression. Behavioral differences between these males are associated with overexpression estrogen receptor alpha in the medial amygdala (MeA) and bed nucleus of the stria terminalis (BST) and neuropeptide expression in the paraventricular nucleus (PVN).

*Corresponding Author: Department of Biological Sciences, University of Texas at El Paso, El Paso 79968, bcushing@utep.edu.

#Co-senior authors

Authors' contributions

All of the authors have contributed substantially to the manuscript.

Concept, drafting and interpretation – Ortiz, Cushing,

Ferris Execution and analysis - Ortiz, Yee, Solomon, Keane, Cai, Kulkarni

Publisher's Disclaimer: This is a PDF file of an unedited manuscript that has been accepted for publication. As a service to our customers we are providing this early version of the manuscript. The manuscript will undergo copyediting, typesetting, and review of the resulting proof before it is published in its final form. Please note that during the production process errors may be discovered which could affect the content, and all legal disclaimers that apply to the journal pertain.

COI: Dr. Ferris reports a financial interest in Animal Imaging Research, the company that makes the RF electronics and holders for animal imaging. Dr. Cushing reported no biomedical financial interests or potential conflicts of interest. Dr. Solomon reported no biomedical financial interests or potential conflicts of interest. Dr. Keane reported no biomedical financial interests or potential conflicts of interest. Dr. Kulkarni reported no biomedical financial interests or potential conflicts of interest. Dr. Yee reported no biomedical financial interests or potential conflicts of interest. Mr. Ortiz reported no biomedical financial interests or potential conflicts of interest. Ms. Cai reported no biomedical financial interests or potential conflicts of interest.

Ethics approval and consent to participate

Not applicable

Consent for publication

Yes

Availability of data and material

All data can be accessed through a link to Mandelley. DOI to follow

Methods: We compared apparent diffusion coefficient (ADC), fractional anisotropy (FA), and BOLD resting-state functional connectivity (rsFC) between males.

Results: IL males displayed higher ADC in regions associated with prosocial behavior including the BST, PVN and the anterior thalamic nuclei, while KI showed higher ADC in the brainstem. KI showed significantly higher FA than IL in 26 brain regions, with the majority being in the brainstem reticular activating system. IL males showed more BOLD-rsFC between the BST, PVN, and MeA along with other brain regions including the hippocampus and areas associated with the social and reward networks.

Conclusion: Our results suggest that gray matter microarchitecture and functional connectivity may play a role the expression of prosocial behavior and suggest that difference in other brain regions, especially in the brainstem, could be involved. The differences between males suggests that this system represents a potential valuable model system for studying emotional differences and vulnerability to stress and addiction.

Keywords

Imaging; BOLD; connectivity; prairie vole; medial amygdala; bed nucleus of the stria terminalis

Introduction

Prairie voles (*Microtus ochrogaster*) are the primary human-relevant rodent model for studying the neural mechanisms and circuits involved in the expression of high levels of prosocial behavior associated with social monogamy. They form long-term pair bonds, express alloparental and biparental offspring care (1), and show depression-like responses to social isolation and partner loss (2). Microtines are a comparative model, as closely related species display a wide spectrum of behavior. Pine (*M. pinetorium*) and prairie voles are socially monogamous and highly prosocial, montane voles (*M. montanus*) are polygynous and solitary, while meadow voles (*M. pennsylvanicus*) display intermediate attributes, but are used as a polygynous model. Studies focusing on voles have provided insight into the neural regulation of prosocial behavior. 1. There are multiple neural mechanisms involved, oxytocin (3,4), vasopressin (5), dopamine (6,7), corticosterone (8) and estrogen receptor expression (9). 2. Two major neural networks, social and reward, as well as other regions/nuclei play a critical role in modulating prosocial behavior (10). 3. The pattern of receptor expression, oxytocin (11), vasopressin (12), estrogen (13), dopamine (14) and corticotrophin-releasing factor (15), vary with reproductive strategy and degree of prosociality. However, we have little or no understanding of the role of higher-brain structure in the generation/regulation of prosocial behavior, which may be critical in modeling human behavior. Therefore, our goal was to test the hypothesis that higher-order brain structure will differ between prosocially distinct males. We tested this by examining the grey matter microarchitecture and resting-state functional connectivity between culturally/behaviorally distinct male prairie voles.

Social monogamy, characterized by high levels of male prosociality and low levels of male/male aggression is based upon Illinois (IL) prairie voles (16). In contrast, Kansas (KS) prairie voles, although socially monogamous (17), display significantly lower levels

of prosocial behavior, less parental (18), form partner preferences with less contact (19) and higher levels of aggression (20) than IL voles. Differential male prosociality is associated with differences in the underlying mechanisms. KS males display significantly less oxytocinergic neurons hypothalamic paraventricular nucleus (PVN) neurons (21) and significantly more estrogen receptor alpha (ER α) in the bed nucleus of the stria terminalis (BST) and the medial amygdala (MeA) than IL males (22). ER α expression is critical, as low levels of BST and MeA ER α is associated with high levels of male prosocial behavior both within and between species (13), as differential ER α expression in MeA and BST is associated with social monogamy in non-microtine rodents (13,23). In IL males enhancement of BST (24) or MeA (9) ER α disrupted prosocial behavior. Conversely, decreasing MeA ER α in male meadow voles increased prosociality and decreased aggression (25). Difference between KS and IL males are exaggerated in F₁ KI males, KS mother/IL father, who have the lowest number of oxytocinergic neurons and more vasopressinergic neurons in the PVN than IL males (21), overexpress BST and MeA ER α (26) and display the lowest levels of prosocial behavior (21). The MeA and BST also play a critical role in social-signal processing, as they receive direct input from the olfactory and accessory olfactory bulbs (27). Given the differences in neuroanatomy and behavior we predicted there would be significant differences between males in grey matter microarchitecture and functional couplings with the BST and MeA between males. Specifically, IL males would show greater BST and MeA connectivity with areas associated with prosocial behavior. Since there are no specific resting-state maps showing overall prosocial functional connectivity (28) we predicted connections with nuclei within the social neural network, i.e. ventromedial hypothalamus, lateral septum, medial preoptic area (MPOA), other amygdaloid nuclei, regions associated with memory and learning, the reward network, i.e frontal cortex, nucleus accumbens (NAc), ventral pallidum or ventral tegmental area in IL males.

Methods

Animal Husbandry

Males originated at the Miami University (Oxford, Ohio, USA) and were transported, 45 to 60 days of age, to the Center for Translational Imaging, Northeastern University (Boston, Massachusetts, USA). Animals were housed with same-sex siblings, PD21, and provided Purina high fiber Rabbit Chow and water *ad libitum*. Animals were housed in a temperature and humidity-controlled vivaria and maintained on a 14/10 light cycle. All procedures were approved by the Miami University and Northeastern University IACUCs prior to conducting any studies and were conducted in accordance with the National Institutes Health Guide for the Care and Use of Laboratory Animals.

Imaging Protocol

A Bruker Biospec 7.0T/20-cm USR horizontal magnet (Bruker, Billerica, MA U.S.A) and a 20-G/cm magnetic field gradient insert (ID=12 cm) was used to scan anesthetized subjects using a quadrature transmit/receive volume coil (ID 38 mm) (29). Imaging sessions began with an anatomical scan (20 slices; slice thickness, 0.70 mm; field of view (FOV) 2.5 cm;

data matrix 256×256; repetition time (TR) 2.5 sec; echo time (TE) 12.0 msec; effective TE 48 msec; number of averages (NEX), 2; total acquisition time, 80 sec).

Diffusion Weighted Imaging–Quantitative Anisotropy

The following procedures were identical to those described previously (30,31). DWI was acquired with a spin-echo echo-planar-imaging (EPI) pulse sequence having the following parameters: TR/TE=500/20 ms, eight EPI segments, and 10 non-collinear gradient directions with a single b-value shell at 1000 s/mm² and one image with a B-value of 0 s/mm² (referred to as B₀). Geometrical parameters were: 48 coronal slices, each 0.313 mm thick (brain volume) and with in-plane resolution of 0.313×0.313 mm² (matrix size 96×96; FOV 30 mm²). The imaging protocol was repeated two times for signal averaging. DWI acquisition took 35–70 min. DWI included DW-3D-EPI images analysis producing fractional anisotropy (FA) maps and apparent diffusion coefficient (ADC). DWI analysis was implemented with MATLAB and MedINRIA (1.9.0;<http://www.sop.inria.fr/asclepios/software/MedINRIA/index.php>) software. Because sporadic excessive breathing can cause motion artifacts apparent only in the slices sampled when motion occurred, each image (for each slice and each gradient direction) was screened, prior to analysis, for motion artifacts; if found, acquisition points with motion artifacts were eliminated from analysis.

For statistical analysis, each brain volume was registered with the 3D MRI Vole Brain Atlas© template (Ekam Solutions LLC, Boston, MA) allowing voxel- and region-based statistics (32). In-house MIVA software was used for image transformations and statistical analyses. For each vole, the B₀ image was co-registered with the B₀ template (using a 6-parameter rigid-body transformation). The co-registration parameters were then applied on the DWI indexed maps for each index of anisotropy. Normalization was performed on the maps providing the most detailed and accurate visualization of brain structures. Normalization parameters were then applied to all indexed maps and then smoothed with a 0.3-mm Gaussian kernel. To ensure that preprocessing did not significantly affect anisotropy values the ‘nearest neighbor’ option was used following registration and normalization. Statistical differences between DWI groups were determined using a Mann-Whitney U Test (α=5%). The formula below was used to account for false discovery from multiple comparisons.

$$P(i) \leq \frac{i}{V} \frac{q}{c(V)}$$

P(i) is the p value based on the t-test analysis. Each of 111 ROIs (i) within the brain containing (V) ROIs was ranked in order of its probability value (Tables S1–S3 Supplement). The false-positive filter value q was set to 0.2 and the predetermined c(V) at unity (33).

Resting-state functional connectivity

The following procedures, with the exception of specific references to voles, were identical to those described previously (30,31). Resting-state fMRI was acquired with a gradient-echo triple-shot EPI sequence, TR/TE 3000/17 ms; matrix size 96×96×20;

voxel size 0.208×0.208×0.75mm; time points 200. Preprocessing was accomplished by combining Analysis of Functional NeuroImages (AFNI_17.1.12, <http://afni.nimh.nih.gov/afni/>), FMRIB Software library (FSL, v5.0.9, <http://fsl.fmrib.ox.ac.uk/fsl/>), Advanced Normalization Tools (ANTs, <https://sourceforge.net/projects/advants/>) and MATLAB (Mathworks, Natick, MA). Brain tissue masks for resting-state functional images were manually drawn using 3DSlicer (<https://www.slicer.org/>) and applied for skull-stripping. Normalization was completed by registering functional data to the MRI vole atlas using affine registration through DRAMMS. This MRI vole brain atlas containing 111 brain regions was used for segmentation. After quality assurance, band-pass filtering (0.01Hz~0.1Hz) was performed, reducing low-frequency drift effects and high-frequency physiological noise. The resulting images were detrended and spatially smoothed (full width at half maximum=0.6 mm). Finally, regressors comprised of motion outliers, the six motion parameters, mean white matter, and cerebrospinal fluid time series were fed into general linear models for nuisance regression removing unwanted effects.

Correlations in spontaneous BOLD fluctuations was measured using region-to-region functional connectivity. Networks consist of nodes and edges; nodes being the brain region of interest (ROI) and edges being the connections between regions. 111 nodes were defined using the ROIs segmented from our vole atlas. Voxel time series data were averaged per node based on the residual images using the nuisance regression procedure with motion parameters and mean time courses of white matter and ventricles. Pearson's correlation coefficients across all node pairs (6105) were computed per subject, assessing temporal correlations between brain areas. r-values (-1 to 1) normality were improved using Fisher's Z-transform. 111×111 symmetric connectivity matrices were constructed, each entry representing the strength of edge. Group-level analysis was performed to examine functional connectivity in all experimental groups. The resulting Z-score matrices from one-group t-tests were clustered using the K-nearest neighbors clustering method to identify how nodes cluster and form resting state networks (see Data in Supplement). A $|Z|=2.3$ threshold was used to avoid spurious or weak node connections for visualization purposes.

Results

Diffusion Weighted Imaging

There were several significant differences in ADC (Table 1 and Fig 1 left column) between males. Many of the differences occurred in the brainstem, e.g. lateral paragigantocellularis, trigeminal complex, facial n., raphe, medullary reticular n. reticulotegmental n. The level of diffusivity, direction of significant difference was region dependent, with IL males being higher in some regions and KI higher in others.

Twenty-six brain areas were significantly different for FA between males. In all cases, FA was higher in KI than IL males (Table 2 and Fig 1 right column). Differences in FA were most prominent in the brainstem reticular activating system, e.g. reticulotegmental n., raphe, gigantocellularis, paragigantocellularis, parvicellular reticular n, pontine reticular n. and medullary reticular n.

Resting-state functional connectivity

Figure 2 shows the rsFC correlation matrix for both males. Letters denote primary clusters constituting major brain regions and their significant connections. IL males showed a greater number of functionally couplings then KI males. These difference are most noted in Area B (insular cortex, olfactory tubercles, medial septum, and BST connecting to rostral piriform, tenia tecta, diagonal band of Broca and medial preoptic), Area D (intra-thalamic connections) and Area G (brainstem reticular activating system).

The correlation matrix was used to generate significant positive correlations with the BST (Fig 3 table), MeA (Fig 4 table), and the PVN (Table 3) with associated Z-score. For all nodes IL males displayed more significant correlations than KI males. In the BST and PVN all KI functional couplings corresponded with IL males. The BST highlights major connectivity differences between males. IL males display extensive connectivity with multiple brain regions, including the amygdala, hypothalamus, basal ganglia e.g., caudate/putamen, NAc, septum, and globus pallidus (Fig 3). IL males also displayed more MeA couplings (Fig 4). Although both KI and IL males showed significant coupling to the surrounding amygdala, only KI was coupled to the central and extended amygdala. IL had coupling to the hypothalamus, NAc shell and the hippocampal complex e.g., CA1, CA3 and dentate. Table 3 shows the limited significant connections associated with the PVN.

Discussion

Our results supported the hypothesis that grey matter microarchitecture and functional coupling would differ between behavioral distinct male prairie voles. Specifically, highly-prosocial IL males had higher FA and greater functional connectivity in regions associated with prosocial behavior and reward than KI males. In contrast, KI males had higher FA in brainstem reticular formations. Our findings are significant because they link mechanisms and regions of the brain known to regulate prosocial behavior with brain microarchitecture and functional connectivity. Although we recognize that many of these brain regions regulated other behaviors and physiological responses our findings are discussed with respect to integrated neural circuitry believed to prosocial behavior and how they might translate to the human condition

Based upon similarities in sociosexual behavior between prairie voles and humans, prairie voles have become the primary human-relevant model for understanding neural regulation of social behavior. They have been used and/or proposed as a translational model for studying depression (34), autism (35,36) and addiction (37,38). Prairie voles, like humans, display significantly different cultural/populational patterns of social behavior and these differences are regulated by significant differences in the underlying mechanism. The differences between Kansas and Illinois prairie vole are well established and robust, supported by decades worth of studies and persist under laboratory conditions after generations of breeding. Additionally, when cross-bred, the sons display maternal behavioral patterns, with KI males displaying overexpression of ER α (26) and reduction in oxytocinergic neurons in the PVN, which is associated with a higher level of aggression and lowest levels of prosocial behavior (25).

It seems a logical extension to consider the KI/IL system as a translational model for fMRI studies. Especially as a predictive model for treatment and assessment of vulnerabilities within and between human populations for mental health disorders and drug abuse. There are challenges to this approach. One involves species differences in processing social cues. Rodents typically use olfaction, while humans rely on vision, meaning that connectivity differs to at least some degree (39). However, the MeA and BST still play a critical role in regulating sociosexual behaviors in all eutherian mammals. Another issue, as eloquently stated in a recent review (28), is that specific-brain regions and functional connectivity associated with regulating prosocial behavior are “inferred” through task-based fMRI studying a single prosocial behavior. Meaning that, in part, because of the complexity, we do not have a “map” of the regions involved, nor do we understand their overall connectivity associated with producing prosociality. This human meta-analysis review examines potential regions involved in prosocial behavior, empathy and mentalizing. Many of the regions that were seen to be different between voles were implicated in the meta-analysis, including the prefrontal cortex and amygdala, with the striatum seen as playing a critical role (28). An interesting experimental approach to overall prosociality was conducted comparing DWI and resting connectivity in humans based upon social network size (40). While not exactly the same, this is comparable to the differential degree of KI/IL male prosociality, with IL males displaying stronger social bonds. There are some interesting correlates with our findings, as social network size was associated with FA in the cingulate cortex (anterior and posterior) and the pre-frontal cortex and greater rsFc within the anterior and posterior cingulate cortex with the amygdala. Drug addiction and resilience are associated with social support and social networks (41), suggesting the KI/IL model could be used in translational drugs of addiction studies. In a human rsFc study resilience was associated with hyperconnectivity in several regions that differed between KI and IL including the prefrontal cortex, caudate nucleus, motor area and putamen (42). If translated to voles would might predict that KI males would be more susceptible to drug addiction.

Grey matter microarchitecture-DWI

The diffusion of water, its directionality and restriction, is complex and dependent upon the microenvironment, i.e. neuronal and glial density, axonal, dendritic and synaptic organization, capillary density, connective tissue, intracellular and extracellular volumes. Given all the postmortem histology reporting cellular and molecular at microscopic levels and reflect gray matter microarchitecture (43). The differential anisotropy we observed shows that there are significant differences in numerous brain areas between the two populational and cultural distinct voles (21,44) we expected to see differences in measures of anisotropy when analyzing 111 brain areas. Indeed, there were many areas that included the olfactory system, basal ganglia and brainstem reticular activating system. The DWI data doesn't assign the difference to one phenotype or the other but simply underscores that they are putative differences in the microanatomy in these different brain areas. The brain areas include the olfactory system which is critical for communication, the basal ganglia required for motivation and goal directed behavior and the reticular activating system which is needed for arousal. Collectively these areas and their interconnections would suggest a difference in behavior or temperament between IL and KI voles.

Grey matter microarchitecture different. In prairie voles social bond formation is regulated by the interaction of two neural networks, social and reward (45), as well as other areas in the limbic system that have afferent or efferent connections with these networks. While further study is required to directly associate differences between prosocial behavior with gray matter microarchitecture and tract density the areas of difference between IL and KI males is very suggestive. IL males displayed significantly higher FA than KI males in regions directly associated to or implicated in the regulation of prosocial behavior, such as the PVN, BST, dorsal raphe nucleus (DRN) and the anterior thalamic n. The PVN produces major neuropeptides, oxytocin, vasopressin and corticotrophin-releasing factor, which regulate the formation of pair bonds (46). The BST plays a major role in the expression of prosocial behavior, including parental behavior and bond formation (24,47,48). The DRN has been associated with the process of the formation of partner preferences. Adult males reared by single mothers, rather than biparentally, showed delays in the formation of partner preferences. These delays were associated with changes in neuropeptide receptors, including in the DRN (49), and through changes in afferent serotonergic neurons from the DRN to the anterior hypothalamus, which modulate aggression and affiliation (50). The anterior thalamic n. plays a role in memory and emotional processing in addition to affective cognition (51), which may play a role in the responses to specific individuals and strength of bonding. ADC was greater in KI males compared with IL males in multiple regions, many of which are in the brain stem. It is difficult to directly link these with specific responses or patterns, but they could be involved in vigilance, aggression, motivation and/or social interactions. They do, however, emphasize the architectural difference between the males, which is further supported by the FA findings.

The FA data reveals several differences in microarchitecture. First, all significant differences were higher in KI FAs, further supporting real differences in brain function between KI and IL males. This supports previous findings that maternal influence is critical in the neuroanatomy of their male offspring (25,26). Males with Kansas mothers have more MeA and BST ER α , with KI males' over-expressing ER α in these areas, but also in the MPOA and ventral medial hypothalamus (26), which regulate sociosexual behavior. It has been hypothesized that male offspring benefit from displaying behavioral and mating patterns associated with their native population, resulting in selection favoring the expression of maternal influences (26). Second, many of the differences are in the brainstem reticular activating system, which is associated with arousal (52) and cognition (53) and could play a role in differential expression of the males' behavioral repertoire. Finally, there are differences in the cortex, prefrontal and anterior cingulate, medial and basal amygdala and NAc core, which are associated with sociosexual behavior, reward and motivation, suggesting that brain architecture is associated with differences in behavior.

Resting-state functional connectivity

As predicted, BOLD rsFc varied significantly between IL and KI males in nuclei/regions that are associated with social behavior, vigilance, reward and motivation. These included the prefrontal cortex, the amygdala, mid-brain reticular formation with the ventral tegmental area and the dorsal raphe and the brainstem reticular activating system, as well as several other regions in intra-thalamic connections, which are associated with signal processing.

rsFC results demonstrate the degree of differences between the males and suggest that understanding connectivity may be a key to understanding the ultimate expression of behavioral differences.

BOLD rsFc has previously been examined in prairie voles, describing base cortical and subcortical networks (27,54). While both studies state that voles are a human-relevant model to understand networks involved in the organization and expression of prosocial behavior, neither presented findings of what these connections/pathways are nor drew conclusions based upon comparisons with other species. While we did do not address the association between functional connectivity and higher order prosocial behavior regulation, i.e. the process of pair bond formation or functional responses of males to their partners, our results do provide insight into the areas of connectivity that may play a critical role because we compared two behaviorally distinct males. The males display significantly different levels of prosocial behavior and aggression (25), which are associated with differential expression of the underlying neural mechanisms (25,26). We analyzed rsFC in the BST, MeA and PVN. These three nuclei play a critical role in regulating social behavior and processing external social stimuli. The PVN is the primary site of central neuropeptides production involved in the expression of prosocial behavior (46). The PVN has efferent connections with nuclei in the social and reward circuits, releasing oxytocin, vasopressin, and corticotrophin-releasing factor. There is also a relationship between the expression of vasopressin and ER α in the PVN that may play a critical role in male prosocial behavior (46). The BST and MeA both receive direct inputs from the olfactory system, with the MeA playing a critical role in social recognition and memory (55). Both nuclei are part of the social neural network (27) and play critical roles in regulating pair bond formation and male paternal behavior (24,47,48). Low levels of ER α in the BST (24) and MeA (9) are essential for the expression of vole male prosocial behavior. Together these studies predict that if male prosocial behavior is associated with higher-order connectivity then these nuclei would be highly likely to have differential connectivity with other regions.

While the study was not designed to relate connectivity with behavioral repertoires the results do suggest an important role of the PVN, BST and MeA. In all three IL males had more significant connections than KI males. In the PVN and BST all the functional connection in KI males occurred in IL males, with IL males having 2x more in the PVN and more than 5x in the BST. In contrast KI and IL shared several connections with the MeA, but KI also displayed connections within the amygdaloid complex, central (CeA) and extended amygdala, not observed in IL. The CeA plays a critical role in fear regulating social interactions (56) suggesting a potential area of interest in regulating KI social interactions. In terms of connectivity with the amygdala IL males show connections with the anterior amygdala from the MeA and BST, while KI males only show significant functional connectivity between the MeA and anterior amygdala. Another region associated with the social neural network, the MPOA (27), is functionally associated with the PVN and BST, but again only in IL males. Multiple node connections were also seen with the NAc, which is involved in motivation and reward. KI and IL males show connectivity between the BST and NAc core, however only IL males displayed connectivity with the NAc shell, MeA and BST. This is an important distinction as the NAc shell, but not the core, is involved in pair bond formation (57). IL males displayed significant connectivity between the anterior

hypothalamus and all three nodes, while KI males only showed connectivity with the MeA. Only IL males displayed PVN/MeA connectivity with the hippocampus. Both nodes being connected with the dentate hippocampus. The dentate hippocampus plays a critical role in learning and memory (58), which is important for social interactions. In addition, IL males showed connectivity of CA1 and CA3 and the MeA. These regions are involved in spatial and contextual memory (59). It should be noted that while KI display significantly lower levels of prosocial behavior they are capable of displaying behaviors associated with social monogamy, suggesting that KI/IL shared nodes of connectivity may be critical for the minimum expression of the necessary prosocial behaviors.

In conclusion, there are significant differences in microarchitecture and resting-state functional connectivity between culturally distinct prairie voles. The findings strongly suggest higher-order brain organization plays a critical role in the expression of prosocial behavior. Further studies are needed to fully understand the structural differences and their role in the expression of prosocial behavior and bond formation, including examining brain architecture in Kansas prairie to understand maternal influence on male offspring brain organization. Finally, our findings suggest that prairie voles are a potentially powerful model for studying microarchitecture, functional connectivity and as a translational rodent model for studying social behavior and social deficit disorders.

Supplementary Material

Refer to Web version on PubMed Central for supplementary material.

Acknowledgements

We wish to thank Connor Lambert and James Lichter for rearing the voles and Nancy Cushing for her comments on drafts of this article.

Funding

Support for this study was provided in part by the Larry P. Jones Distinguished Professorship Endowment through The University of Texas El Paso (BSC), NICHD HD75222 (BK, NGS, BSC) and NIH MIGMS 5R25GM069621-17 (in support of RJO).

References

1. Mech S, Dunlap A, Hodges K, Wolff J (2002): Multi-male mating by paired and unpaired female prairie voles (*Microtus ochrogaster*). *Behaviour* 139: 1147–1160.
2. Grippo AJ, Cushing BS, Carter CS (2007): Depression-like behavior and stressor-induced neuroendocrine activation in female prairie voles exposed to chronic social isolation. *Psychosom Med* 69: 149–157. [PubMed: 17289829]
3. Insel TR, Hulihan TJ (1995): A gender-specific mechanism for pair bonding: oxytocin and partner preference formation in monogamous voles. *Behav Neurosci* 109: 782–789. [PubMed: 7576222]
4. Williams JR, Carter CS, Insel T (1992): Partner preference development in female prairie voles is facilitated by mating or the central infusion of oxytocin. *Ann Ny Acad Sci* 652: 487–9. [PubMed: 1626857]
5. Tickerhoof MC, Smith AS (2017): Vasopressinergic neurocircuitry regulating social attachment in a monogamous species. *Front Endocrinol* 8: 265.

6. Aragona BJ, Liu Y, Curtis JT, Stephan FK, Wang Z (2003): A critical role for nucleus accumbens dopamine in partner-preference formation in male prairie voles. *J Neurosci* 23: 3483–3490. [PubMed: 12716957]
7. Wang Z, Yu G, Cascio C, Liu Y, Gingrich B, Insel TR (1999): Dopamine D2 receptor-mediated regulation of partner preferences in female prairie voles (*Microtus ochrogaster*): A mechanism for pair bonding? *Behav Neurosci* 113: 602–611. [PubMed: 10443786]
8. DeVries AC, DeVries MB, Taymans S, Carter CS (1995): Modulation of pair bonding in female prairie voles (*Microtus ochrogaster*) by corticosterone. *Proc National Acad Sci* 92: 7744–7748.
9. Cushing BS, Perry A, Musatov S, Ogawa S, Papademetriou E (2008): Estrogen receptors in the medial amygdala inhibit the expression of male prosocial behavior. *J Neurosci* 28: 10399–10403. [PubMed: 18842899]
10. Walum H, Young LJ (2018): The neural mechanisms and circuitry of the pair bond. *Nat Rev Neurosci* 19: 643–654. [PubMed: 30301953]
11. Insel TR, Shapiro LE (1992): Oxytocin receptor distribution reflects social organization in monogamous and polygamous voles. *Proc National Acad Sci* 89: 5981–5985.
12. Insel T, Wang Z, Ferris C (1994): Patterns of brain vasopressin receptor distribution associated with social organization in microtine rodents. *J Neurosci* 14: 5381–5392. [PubMed: 8083743]
13. Cushing BS, Wynne-Edwards KE (2006): Estrogen receptor- α distribution in male rodents is associated with social organization. *J Comp Neurol* 494: 595–605. [PubMed: 16374794]
14. Smeltzer MD, Curtis JT, Aragona BJ, Wang Z (2006): Dopamine, oxytocin, and vasopressin receptor binding in the medial prefrontal cortex of monogamous and promiscuous voles. *Neurosci Lett* 394: 146–151. [PubMed: 16289323]
15. Lim MM, Nair HP, Young LJ (2005): Species and sex differences in brain distribution of corticotropin-releasing factor receptor subtypes 1 and 2 in monogamous and promiscuous vole species. *J Comp Neurology* 487: 75–92.
16. Getz LL, Carter CS, Gavish L (1981): The mating system of the prairie vole, *Microtus ochrogaster*: Field and laboratory evidence for pair-bonding. *Behav Ecol Sociobiol* 8: 189–194.
17. Thomas JA, Birney EC (1979): Parental care and mating system of the prairie vole, *Microtus ochrogaster*. *Behav Ecol Sociobiol* 5: 171–186.
18. Roberts RL, Williams JR, Wang AK, Carter CS (1998): Cooperative breeding and monogamy in prairie voles: influence of the sire and geographical variation. *Anim Behav* 55: 1131–1140. [PubMed: 9632499]
19. Cushing BS, Martin JO, Young LJ, Carter CS (2001): The effects of peptides on partner preference formation are predicted by habitat in prairie voles. *Horm Behav* 39: 48–58. [PubMed: 11161883]
20. Gaines MS, Fugate CL, Johnson ML, Johnson DC, Hisey JR, Quadagno DM (1985): Manipulation of aggressive behavior in male prairie voles (*Microtus ochrogaster*) implanted with testosterone in silastic tubing. *Can J Zool* 63: 2525–2528.
21. Stetzk L, Payne RE, Roache LE, Ickes JR, Cushing BS (2018): Maternal and paternal origin differentially affect prosocial behavior and neural mechanisms in prairie voles. *Behav Brain Res* 360: 94–102. [PubMed: 30521929]
22. Cushing BS, Razzoli M, Murphy AZ, Epperson PM, Le W-W, Hoffman GE (2004): Intraspecific variation in estrogen receptor alpha and the expression of male sociosexual behavior in two populations of prairie voles. *Brain Res* 1016: 247–254. [PubMed: 15246861]
23. Cushing BS (2016): Estrogen receptor alpha distribution and expression in the social neural network of monogamous and polygynous *Peromyscus*. *PLoS One* DOI: 10.1371/journal.pone.0150373 PMID: 41. Newman SW (1999): The medial extended amygdala in male reproductive behavior a node in the mammalian social behavior network. *Ann NY Acad Sci* 877: 242–257. [PubMed: 10415653]
24. Lei K, Cushing BS, Musatov S, Ogawa S, Kramer KM (2010): Estrogen receptor- α in the bed nucleus of the stria terminalis regulates social affiliation in male prairie voles (*Microtus ochrogaster*). *Plos One* 5: e8931. [PubMed: 20111713]
25. Stetzk L, Ganshevsky D, Lende MN, Roache LE, Musatov S, Cushing BS (2018): Inhibiting ER α expression in the medial amygdala increases prosocial behavior in male meadow voles (*Microtus pennsylvanicus*). *Behav Brain Res* 351: 42–48. [PubMed: 29859197]

26. Kramer KM, Carr MS, Schmidt JV, Cushing BS (2006): Parental regulation of central patterns of estrogen receptor α . *Neuroscience* 142: 165–173. [PubMed: 16876954]
27. Newman SW (1999): The medial extended amygdala in male reproductive behavior a node in the mammalian social behavior network. *Ann NY Acad Sci* 877: 242–257. [PubMed: 10415653]
28. Bellucci G, Camilleri JA, Eickhoff SB, Krueger F (2020): Neural signatures of prosocial behaviors. *Neurosci Biobehav Rev* 118: 86–195. doi: 10.1016/j.neubiorev.2020.07.006
29. Ferris CF, Kulkarni P, Toddes S, Yee J, Kenkel W, Nedelman M (2014): Studies on the Q175 knock-in model of Huntington's disease using functional imaging in awake mice: Evidence of Olfactory Dysfunction. *Front Neurol* 5: 94. [PubMed: 25071696]
30. Ferris CF, Sarah Nodinea S, Trent Pottalaa T, Xuezhua Caia X, Tatiana M. Knoxa TM, Fanta H. Fofana F, et al. (2019): Alterations in brain neurocircuitry following treatment with the chemotherapeutic agent paclitaxel in rats. *Neurobiol Pain* 6: 10.1016/j.nypai.2019.100034
31. Kulkarnia P, Grantf S, Morrisona TR, Caia X, Iriaha S, Kristal BS, et al. (2020): Characterizing the human APOE epsilon 4 knock-in transgene in female and male rats with multimodal magnetic resonance imaging. *Brain Res* 1747: preprint 10.1016/j.brainres.2020.147030
32. Yee JR, Kenkel WM, Kulkarni P, Moore K, Perkeybile AM, Toddes S, et al. (2016): BOLD fMRI in awake prairie voles: A platform for translational social and affective neuroscience. *Neuroimage* 138: 221–32. [PubMed: 27238726]
33. Benjamini Y, Hochberg Y (1995): Controlling the false discovery rate: a practical and powerful approach to multiple testing. *J Royal Statistical Soc Ser B Methodol* 57: 289–300.
34. Grippo AJ, Cushing BS, Carter CS (2007): Social isolation induces depression- and anxiety-like behaviors and neuroendocrine dysfunction in prairie voles. *Psychosomatic Medicine* 69:149–157. [PubMed: 17289829]
35. Green JG, Hollander E (2010): Autism and oxytocin: New developments in translational approaches to therapeutics. *Neurotherapeutics* 7:250–257. Aragona BJ, Detwiler JM, Wang Z (2007): Amphetamine reward in the monogamous prairie vole. *Neurosci Lett* 22:
36. Horie K, Kiyoshi I, Suzuki S, Adachi S, Yada S, Hirayama T, Hidema S, Young LJ, Nishimori K (2019): Oxytocin receptor knockout prairie voles generated by CRISPR/Cas9 editing show reduced preference for social novelty and exaggerated repetitive behaviors. *Horm Behav* 111:60–69. 10.1016/j.yhbeh.2018.10.011 [PubMed: 30713102]
37. Aragona BJ, Detwiler JM, Wang Z (2007) Amphetamine reward in the monogamous prairie vole. *Neurosci Lett* 418:190–194. [PubMed: 17400384]
38. Hostetler CM, Anacker AMJ, Loftis JM, Ryabinin AE (2012): Social housing and alcohol drinking in male-female pairs of prairie voles (*Microtus ochrogaster*). *Psychopharmacol* 224:121–132.
39. Zink CF, Meyer-Lindenberg A (2012): Human neuroimaging of oxytocin and vasopressin in social cognition. *Horm Behav* 61:400–409. doi:10.1016/j.yhbeh.2012.01.016. [PubMed: 22326707]
40. Noonan MP, Mars RB, Sallet J, Dunbar RIM, Fellows LK (2018): The structural and functional brain networks that support human social networks. *Behav Brain Res* 355:12–23.
41. Yang C, Xia M, Han M, Liang Y (2018): Social support and resilience as mediators between stress and life satisfaction among people with substance use disorder in China. *Front Psych* 10:3389/fpsy.2018.00436
42. Ersche KD, Menga C, Ziauddeena H, Stochla J, Williamse GB, Bullmore ET, Robbins TW (2020): Brain networks underlying vulnerability and resilience to drug addiction. *Proc Nat Acad Sci USA* 117: 15253–15261. [PubMed: 32541059]
43. Cushing BS, Kramer KM (2005): Microtines: A model system for studying the evolution and regulation of social monogamy. *Acta Theriol Sinica* 25: 182–199.
44. Kulkarni P, Kenkel W, Finklestein SP, Barchet TM, Ren J, Davenport M, et al. (2015): use of anisotropy, 3d segmented atlas, and computational analysis to identify gray matter subcortical lesions common to concussive injury from different sites on the cortex. *Plos One* 10: e0125748. [PubMed: 25955025]
45. Young KA, Gobrogge KL, Liu Y, Wang Z (2010): The neurobiology of pair bonding: insights from a socially monogamous rodent. *Front Neuroendocrin* 32: 53–69.

46. Kramer KM, Yamamoto Y, Hoffman GE, Cushing BS (2005): Estrogen receptor α and vasopressin in the paraventricular nucleus of the hypothalamus in *Peromyscus*. *Brain Res* 1032: 154–161. [PubMed: 15680954]
47. Wang Z, Smith W, Major DE, Vries GJD (1994): Sex and species differences in the effects of cohabitation on vasopressin messenger RNA expression in the bed nucleus of the stria terminalis in prairie voles (*Microtus ochrogaster*) and meadow voles (*Microtus pennsylvanicus*). *Brain Res* 650: 212–218. [PubMed: 7953686]
48. Numan M, Insel TR (2003): Paternal Behavior. In: *The Neurobiology of Parental Behavior*, vol. 1. New York: Springer.
49. Ahern TH, Young LJ (2009): The impact of early life family structure on adult social attachment, alloparental behavior, and the neuropeptide systems regulating affiliative behaviors in the monogamous prairie vole (*Microtus ochrogaster*). *Front Behav Neurosci* 3: 17. [PubMed: 19753327]
50. Gobrogge KL, Jia X, Liu Y, Wang Z (2017): neurochemical mediation of affiliation and aggression associated with pair-bonding. *Biol Psychiat* 81: 231–242. [PubMed: 27129413]
51. Dupire A, Kant P, Mons N, Marchand AR, Coutureau E, Dalrymple-Alford J, Wolff M (2013): A role for anterior thalamic nuclei in affective cognition: interaction with environmental conditions. *Hippocampus* 23: 392–404. [PubMed: 23436341]
52. Saper CB, Scammell TE, Lu J (2005): Hypothalamic regulation of sleep and circadian rhythms. *Nature* 437: 1257–1263. [PubMed: 16251950]
53. De Cicco V, Fantozzi MPT, Cataldo E, Barresi M, Bruschini L, Faraguna U, Manzoni D (2017): Trigeminal, visceral and vestibular inputs may improve cognitive functions by acting through the locus coeruleus and the ascending reticular activating system: a new hypothesis. *Front Neuroanat* 11: 130. [PubMed: 29358907]
54. Ortiz JJ, Portillo W, Paredes RG, Young LJ, Alcauter S (2018): Resting state brain networks in the prairie vole. *Sci Rep* 8: 1231. [PubMed: 29352154]
55. Ferguson JN, Aldag JM, Insel TR, Young LJ (2001): Oxytocin in the medial amygdala is essential for social recognition in the mouse. *J Neurosci* 21: 8278–8285. [PubMed: 11588199]
56. LeDoux JE (2000): Emotion circuits in the brain. *Ann Rev Neurosci* 23: 155–184. [PubMed: 10845062]
57. Aragona BJ, Liu Y, Yu YJ, Curtis JT, Detwiler JM, Insel TR, Wang Z (2006): Nucleus accumbens dopamine differentially mediates the formation and maintenance of monogamous pair bonds. *Nat Neurosci* 9: 133–139. [PubMed: 16327783]
58. Kesner RP (2007): A behavioral analysis of dentate gyrus function. *Progress in Brain Research* 163: 567–576. [PubMed: 17765738]
59. Vazdarjanova A, Guzowski JF (2004): Differences in hippocampal neuronal population responses to modifications of an environmental context: evidence for distinct, yet complementary, functions of CA3 and CA1 ensembles. *J Neurosci* 24: 6489–6496. [PubMed: 15269259]

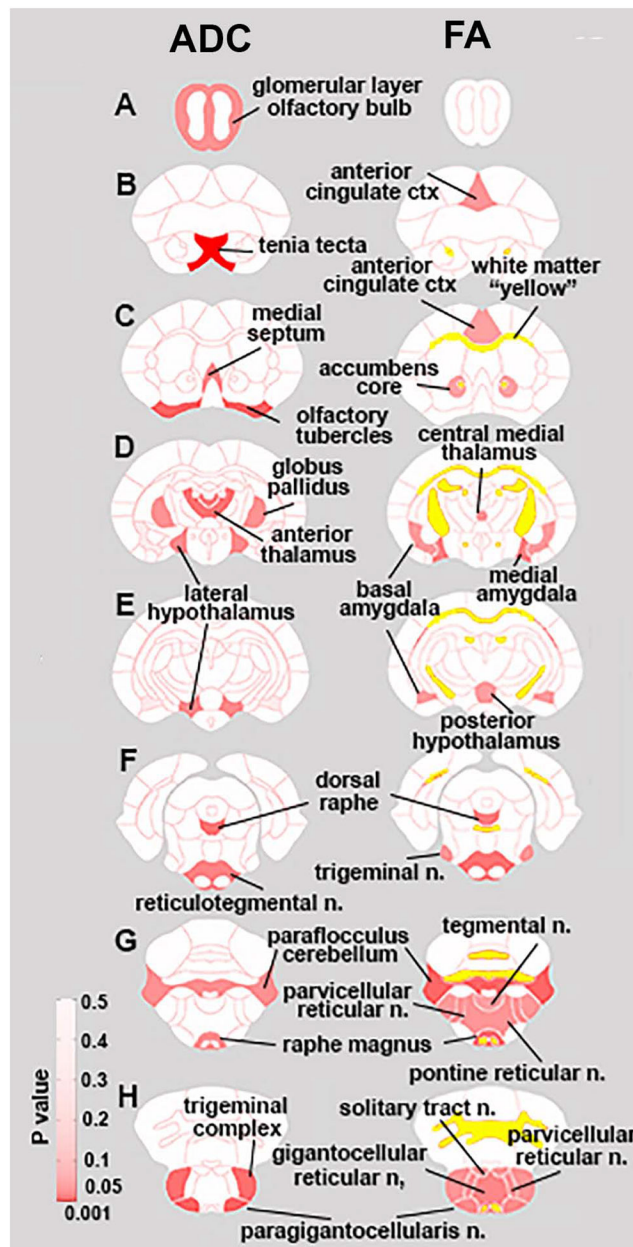


Figure 1. Diffusion Weighted Imaging. Left hand column shows regions of significant differences in Apparent Diffusion Coefficients (ADC) between IL and KI males, while the right hand column indicates regions with significant differences in Fractional Anisotropy. P values (.047 ADC, .045 FA) for brain regions are indexed by degree of red shading, while significant differences in white matter are indicated in yellow.

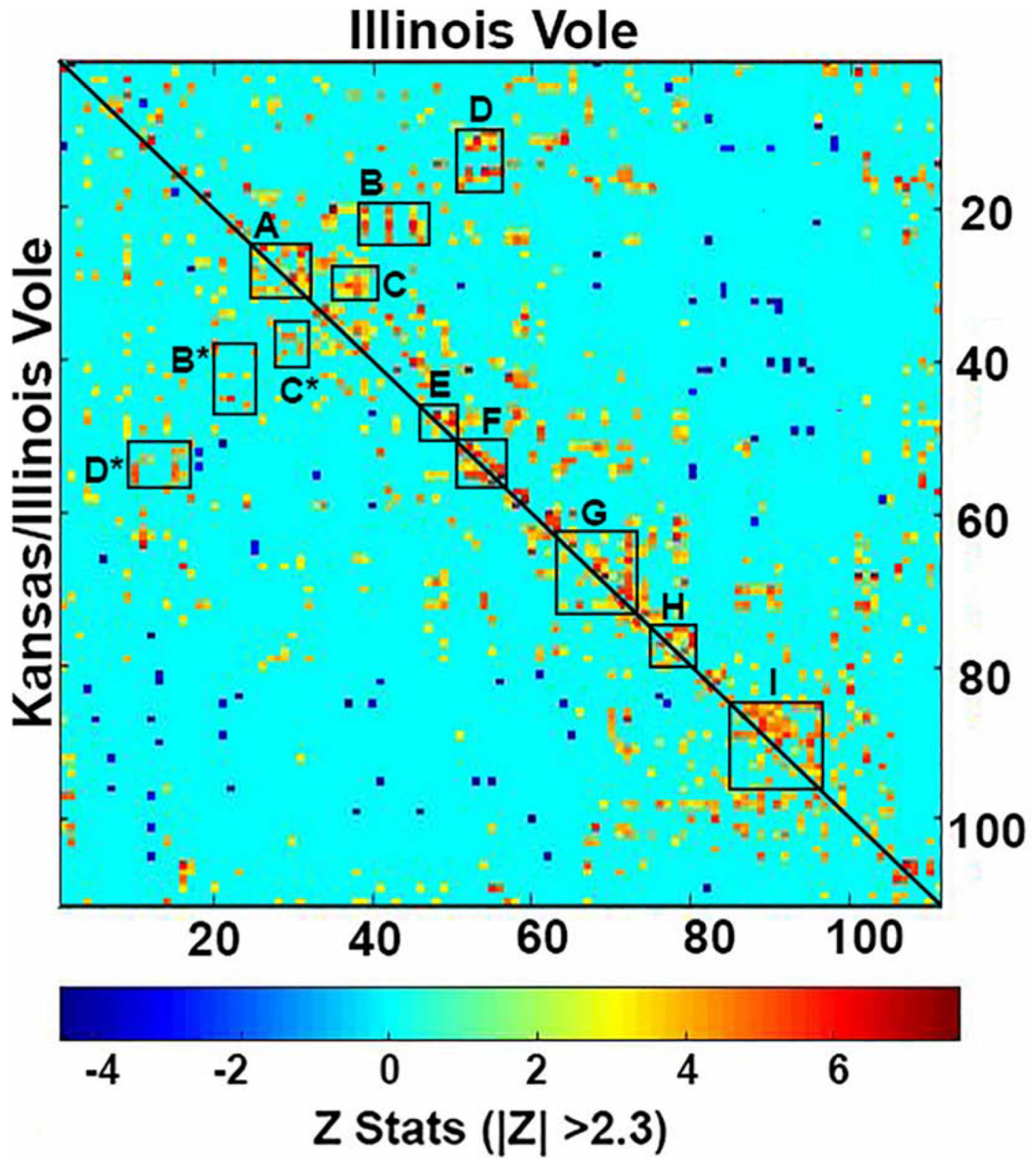


Figure 2. Shows Resting-state functional connectivity. Upper left graph is a correlation matrices of rsfc between IL (top/right) and KI (left/bottom) males separated by the diagonal line. Each colored red/orange pixel represents 1 of 111 brain areas that has a significant positive correlation with other brain areas. Pixels in shades of blue have a significant negative, or anticorrelation with other brain regions. The brain areas with significant correlations appear as clusters because they are contiguous in their neuroanatomy and function. Each pixel on one side of the line has a mirror image pixel on the other side. The delineated areas serve to focus attention on similarities and differences in connectivity. For example, the rectangles labeled B and B* highlight the differences between IL and KI, respectively. The brain areas outlined by the rectangles include the insular ctx, olfactory tubercles, medial septum and

BST and their connections with the rostral piriform, tenia tecta, diagonal band of Broca and medial preoptic n. Significant correlations passing the $|Z| > 2.3$ threshold are shown.

Area A – Prefrontal ctx e.g. prelimbic, infralimbic, association, orbital, ant cingulate

Area B - Lines highlighting box are the insular cortex, olfactory tubercles, medial septum, and bed n. stria terminalis connecting to rostral piriform, tenia tecta, diagonal band of Broca and medial preoptic

Area C – caudate putamen, somatosensory ctx, claustrum, endopiriform ctx connecting to 2nd primary motor cortices and orbit ctx

Area D – Intra-thalamic connections

Area E – Amygdala

Area F – Thalamus

Area G – highlighted by line which is midbrain reticular formation making connections with VTA, SN, PAG, dorsal raphe, posterior hypothalamus, medial geniculate red nucleus

Area H – anterior cerebellum and subiculum and entorhinal ctx

Area I – brainstem reticular activating system – pontine reticular n., tegmental n., parabrachial n., trigeminal complex, paraflocculus, gigantocellularis, reticulotegmental n., parvicellular reticular n.

The pixel positions describe are mirror images of each other with a diagonal line separating IL and KI groups. Z-scores of Pearson's correlation coefficients are displayed in a color-coded matrix for both groups, with the greater absolute Z value indicating greater connections between two region pairs and smaller absolute values indicating weaker connections. Delineated brain regions with significant correlations are clustered based on their contiguous neuroanatomy and/or function.

Numerous neural regions (labeled A-I) are highlighted and magnified displaying the differences in connectivity.

Connections with Bed Nucleus Stria Terminalis

Bed n. Stria Terminalis	Illinois Z score	Kansas Illinois Z score
lateral preoptic area	3.4	-
medial preoptic area	2.5	-
diagonal band of Broca	2.5	-
anterior amygdala	3.1	-
extended amygdala	3.2	3.4
lateral hypothalamus	3.4	-
anterior hypothalamus	2.5	-
caudate/putamen	2.7	-
accumbens core	4.0	2.6
accumbens shell	2.7	-
lateral septum	3.5	-
medial septum	2.7	-
globus pallidus	3.4	-
anterior thalamus	3.1	2.4
retrosplenial ctx	2.3	-
agranular insular ctx	2.4	-

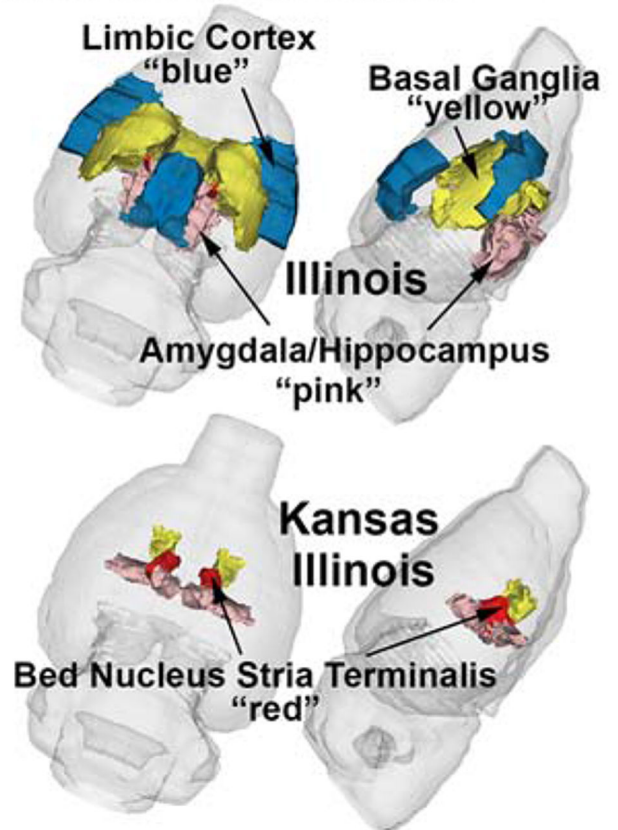


Figure 3. Compares the significant functional connectivity with the BST between IL and KI males. The colors in the 3D graphics indicate areas that show regions with higher functional connectivity in both populations. Embedded tables show significant ($|Z| > 2.3$), while “-” indicates ns) resting-state functional connections.

Connections with Medial Amygdala

Medial Amygdala	Illinois Z score	Kansas Illinois Z score
cortical amygdala	3.5	2.6
central amygdala	-	2.7
basal amygdala	3.2	3.1
anterior amygdala	3.4	2.7
extended amygdala	-	2.3
lateral hypothalamus	3.1	2.4
anterior hypothalamus	2.6	-
n. lateral olfactory tract	2.4	2.8
interpeduncular n.	2.6	-
accumbens shell	2.4	-
CA1 hippocampus	2.7	-
CA3 hippocampus	2.6	-
dentate hippocampus	2.4	-
visual ctx	-	3.2

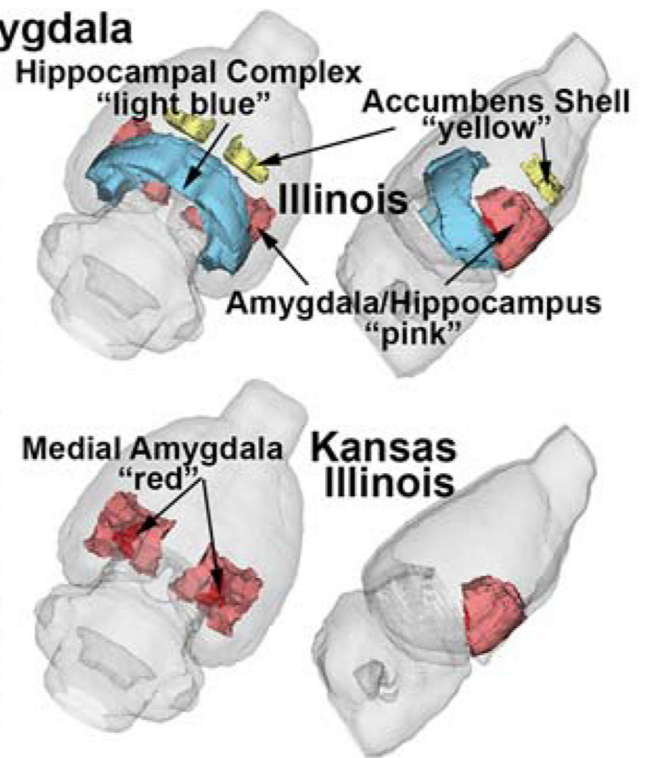


Figure 4.

Compares the significant functional connectivity with the MeA between IL and KI males.

The colors in the 3D graphics indicate areas that show regions with higher functional connectivity in both populations. Embedded table show significant ($|Z| > 2.3$), while “-” indicates ns) resting-state functional connections.

Table 1.

Shows the apparent diffusion coefficient, average + SD, of the 19 areas regions, out of 111 brain areas in the vole MRI atlas, that were significantly different between IL and KI males. Regions are presented in order of significant differences. A significance level of $p = 0.034$ was applied to adjust for multiple comparisons.

Apparent Diffusion Coefficient						
Brain Area	Illinois			Kansas/Illinois		
	AVG	SD		AVG	SD	P-val
tenia tecta ctx	1.43	0.13	<	1.81	0.17	0.001
lateral paragigantocellular nucleus	0.42	0.54	<	1.47	0.85	0.011
olfactory tubercles	1.40	0.34	<	1.95	0.43	0.012
trigeminal complex medulla	0.62	0.35	<	1.01	0.21	0.017
facial nucleus medulla	0.29	0.37	<	1.13	0.80	0.018
dorsal raphe	1.24	0.11	>	1.12	0.05	0.019
anterior thalamic nuclei	1.22	0.13	>	1.08	0.07	0.020
paraventricular nucleus	1.28	0.17	>	1.11	0.09	0.026
medullary reticular nucleus	0.67	0.53	<	1.26	0.42	0.028
reticulotegmental nucleus	0.40	0.41	<	0.90	0.40	0.028
bed nucleus stria terminalis	1.19	0.10	>	1.09	0.05	0.030
ventral tegmental area	1.08	0.39	<	1.58	0.44	0.031
lateral dorsal thalamic nucleus	1.31	0.11	>	1.20	0.07	0.033
lateral hypothalamus	1.17	0.32	<	1.49	0.21	0.035
medial septum	1.22	0.10	>	1.12	0.06	0.036
paraflocculus cerebellum	0.81	0.32	<	1.23	0.41	0.038
raphe magnus	0.54	0.74	<	1.48	0.91	0.040
glomerular layer olfactory bulb	0.97	0.44	<	1.39	0.31	0.044
globus pallidus	1.15	0.10	>	1.06	0.06	0.045

Table 2.

Shows the average \pm SD fractional anisotropy in 26 regions in which there was a significant difference between IL and KI males. In all case KI was higher than IL males. Regions are presented in rank order of significance. A significance level of $p = 0.047$ was applied when taking into consideration multiple comparisons.

Fractional Anisotropy						
Brain Area	Illinois		<	Kansas/Illinois		P-val
	AVG	SD		AVG	SD	
red nucleus	0.46	0.04	<	0.53	0.04	0.002
white matter	0.50	0.04	<	0.55	0.03	0.004
lateral preoptic area	0.51	0.05	<	0.58	0.02	0.006
paraflocculus cerebellum	0.29	0.11	<	0.42	0.04	0.009
facial nucleus medulla	0.07	0.09	<	0.24	0.14	0.011
raphe magnus	0.11	0.17	<	0.37	0.18	0.012
reticulotegmental nucleus	0.12	0.13	<	0.30	0.12	0.013
reticular formation	0.45	0.04	<	0.51	0.04	0.017
dorsal raphe	0.48	0.04	<	0.54	0.05	0.017
medial amygdala	0.46	0.11	<	0.56	0.04	0.018
gigantocellular reticular nucleus	0.26	0.22	<	0.49	0.10	0.020
vestibular nucleus	0.39	0.17	<	0.54	0.04	0.023
lateral paragigantocellular nucleus	0.11	0.16	<	0.32	0.17	0.023
trigeminal complex medulla	0.22	0.14	<	0.36	0.10	0.030
prelimbic ctx	0.35	0.05	<	0.40	0.05	0.030
parvicellular reticular nucleus	0.30	0.19	<	0.48	0.09	0.031
pontine reticular nucleus caudal	0.34	0.18	<	0.51	0.08	0.032
solitary tract nucleus	0.32	0.21	<	0.50	0.06	0.035
trigeminal complex pons	0.27	0.14	<	0.41	0.10	0.036
central medial thalamic nucleus	0.44	0.05	<	0.50	0.05	0.037
posterior hypothalamus	0.46	0.10	<	0.55	0.05	0.040
basal amygdala	0.48	0.06	<	0.55	0.06	0.041
anterior cingulate ctx	0.40	0.02	<	0.45	0.06	0.042
tegmental nucleus	0.46	0.12	<	0.56	0.05	0.043
accumbens core	0.49	0.04	<	0.54	0.04	0.046
medullary reticular nucleus	0.24	0.21	<	0.44	0.15	0.047

Table 3.

Shows significant ($|Z| > 2.3$) resting-state couplings (“-“ indicates ns) with the paraventricular nucleus of the hypothalamus in IL and KI males.

Paraventricular Nucleus	Illinois Z score	Kansas Illinois Z score
reuniens thalamus	3.5	3.5
dorsomedial hypothalamus	3.8	4.1
anterior hypothalamus	4.0	3.6
medial preoptic area	3.0	-
tenia tecta	2.4	-
dentate hippocampus	2.4	-

Author Manuscript

Author Manuscript

Author Manuscript

Author Manuscript